

Micro/nanofluidic devices for drug delivery

Navid Kashaninejad^{a,*}, Ehsanollah Moradi^b, and Hajar Moghadas^c

^aQueensland Micro- and Nanotechnology Centre, Nathan Campus, Griffith University, Brisbane, QLD, Australia

^bDepartment of Biomedical Engineering, Amirkabir University of Technology, Tehran, Iran

^cDepartment of Mechanical Engineering, Gas and Petroleum Faculty, Yasouj University, Yasuj, Iran

*Corresponding author: e-mail address: n.kashaninejad@griffith.edu.au

Contents

1. Microfluidic <i>in vitro</i> drug delivery at the cellular level	2
1.1 Microfluidic concentration gradient generators (MCGGs)	2
1.2 Gradient generators for high-throughput drug screening	8
1.3 Challenges and possible solutions for microfluidic drug delivery at cellular level	11
2. Microfluidic <i>in vitro</i> drug delivery at tissue level	12
3. Microfluidic <i>in situ</i> drug delivery at organ level	19
3.1 Solid microneedles	22
3.2 Coated microneedles	22
3.3 Dissolvable microneedles	23
3.4 Hollow microneedles	24
3.5 Swollen microneedles	24
3.6 Challenge of microneedle drug delivery systems	24
4. Conclusion and future perspective	25
References	26

Abstract

Micro/nanofluidic drug delivery systems have attracted significant attention as they offer unique advantages in targeted and controlled drug delivery. Based on the desired application, these systems can be categorized into three different groups: *in vitro*, *in situ* and *in vivo* microfluidic drug delivery platforms. *In vitro* microfluidic drug delivery platforms are closely linked with the emerging concept of lab-on-a-chip for cell culture studies. These systems can be used to administer drugs or therapeutic agents, mostly at the cellular or tissue level, to find the therapeutic index and can potentially be used for personalized medicine. *In situ* and *in vivo* microfluidic drug delivery platforms are still at the developmental stage and can be used for drug delivery at tissue or organ levels. A famous example of these systems are microneedles that can be used for painless

and controllable delivery of drugs or vaccines through human skin. This chapter presents the cutting edge advances in the design and fabrication of *in vitro* microfluidic drug delivery systems that can be used for both cellular and tissue drug delivery. It also briefly discusses the *in situ* drug delivery platforms using microneedles.



1. Microfluidic *in vitro* drug delivery at the cellular level

Drug delivery has different stages in the body, and dissolvable drug molecules go through a process that finally ends up with delivering the drug molecules to the site of interest and taking up the drug by the targeted cells; therefore, drug delivery experiments at the cellular level are of great importance and commonly applied for the study of cytotoxicity testing, drug screening and drug discovery.¹ In the last decade, various *in vitro* cell culture platforms have been developed for drug screening and development practices. Although these conventional methods are cost-efficient, robust, and easy to manipulate, they lack a physiologically-relevant microenvironment, sustained cell viability, and functional stability. Hence, there is a dire need in the drug development pipeline for developing predictive *in vitro* models with high preclinical efficacy that faithfully recapitulate cell-cell interactions and cellular phenotype.^{2–6}

Microfluidic systems offer a high surface-to-volume ratio that gives rise to unique surface-dominating phenomena such as slip flow.⁷ Surface-dominated forces in microfluidic systems offer significant advantages for drug delivery application. For instance, the laminar and diffusion-based flow in microchannels can precisely control the mechanism of drug release.

Recently, microtechnologies and microfluidic cell culture systems have paved the way for examining complex biologic processes, and with controlling spatiotemporal parameters, they can mimic the intricate cellular micro-environment properties like cell morphology, cell-drug interactions, and chemical concentration gradients.^{6,8} Microfluidic devices can offer chemical concentration gradients with great accuracy and sensitivity, ideal for producing controllable drug profiles and evaluating concentration-dependent cellular responses to different drug doses.^{1,9–11}

1.1 Microfluidic concentration gradient generators (MCGGs)

Microfluidic concentration gradient generators, unlike traditional platforms, possess extraordinary characteristics like cost-efficient operation, the ability to generate accurate and flexible drug profiles, allow real-time cellular

response monitoring, and offer high-throughputs.^{1,12} Microfluidic concentration gradient generators are generally divided into diffusion-based and flow-based platforms and have become an essential tool for studying biological phenomena like cell migration, proliferation, chemotaxis, drug screening, and personalized medicine.^{1,13,14} The following section overview different cell-based MCGGs for drug testing experiments.

1.1.1 Diffusion-based gradient generators

The diffusion base method's gradient generators mostly consist of a membrane or hydrogel to create an environment suitable for diffusive transport.^{12,15} There are two compartments with high and low reagent concentrations in most cases, and the targeted cells are cultured in the bridging channel between the source and the sink.¹ In one study, a shear stress-free MCGG was developed for studying cytoskeleton dynamics molecular pathways and the effect of the Cytochalasin D gradient on MG-63 cellular response.¹⁶ In this study, a profile of Cytochalasin D concentration ranging between 0 and 5 $\mu\text{g/mL}$ was produced in five independent cell chambers, and the concentration-dependent cell responses were examined by measuring cell area and cell eccentricity.¹⁶

Different biological phenomena like chemotaxis and morphogenesis are driven by essential cell signaling cues that are often delivered by biochemical concentration gradients.^{17,18} A microfluidic biochip was developed in one study for generating diffusion-based orthogonal linear concentration gradients in a 3D hydrogel-based scaffold in two different designs: Simultaneous and Sequential (Fig. 1A).¹⁸ It was demonstrated that the two orthogonal gradients of retinoic acid and smoothened agonist emulated the localized differentiation of stem cells, and the neural tube was preferentially developed in the high morphogens concentration regions. Moreover, HT1080, as a highly metastatic fibrosarcoma cell line, was exposed to a rotating gradient of Fetal Bovine Serum (FBS) for probing chemotactic response time and adaptation in the tumor microenvironment. The direction of cell migration and cell's migratory behavior was evaluated by comparing average cell displacements, distribution, and migration speed.¹⁸

In work done by Kilinc et al., a diffusion-based microchip was constructed to establish multiple compounds linear concentration gradient over different cells for cell-based drug combination assays.¹⁹ The microfluidic tool consisted of a cell culture chamber and parallel flow channels for creating a linear concentration gradient across the chamber. Producing orthogonally-aligned gradients of two compounds, flowing concentrated

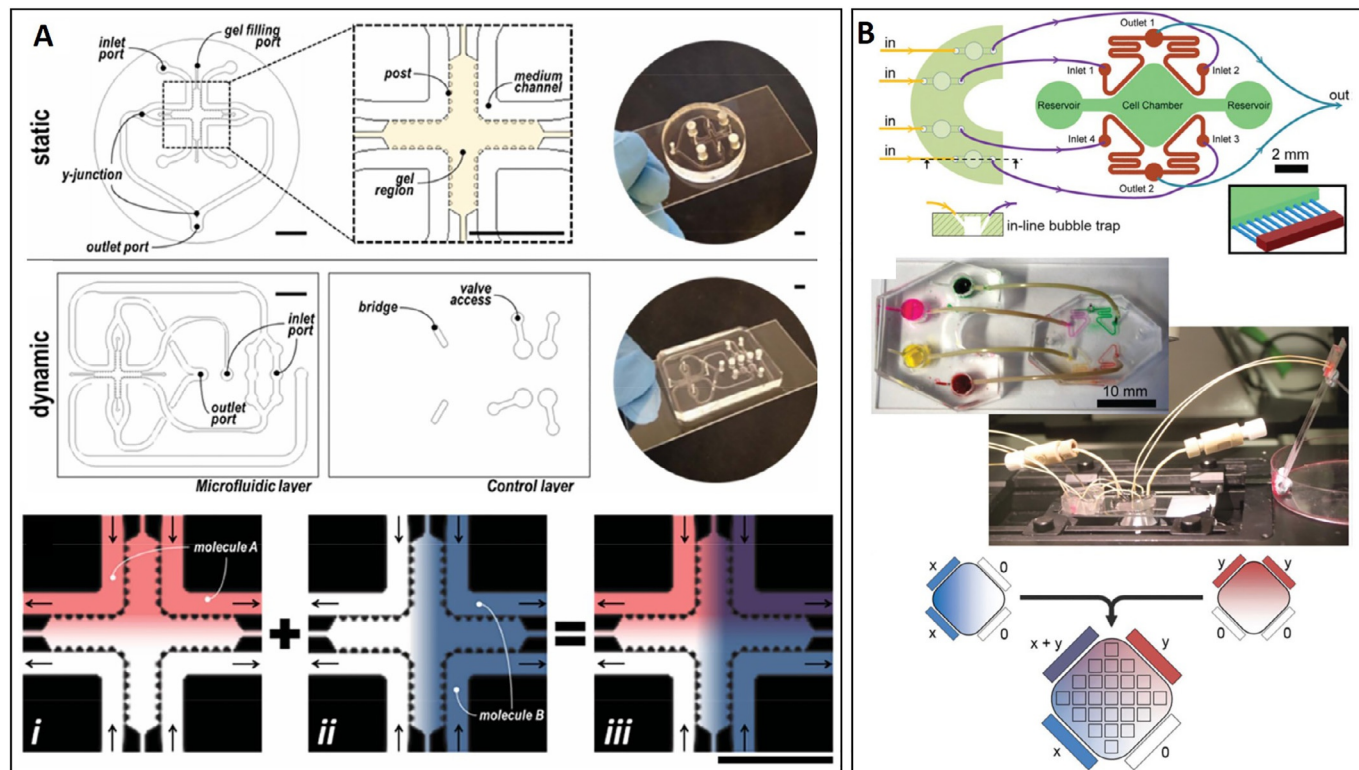


Fig. 1 See figure legend on opposite page.

solutions in two perpendicular directions is needed (Fig. 1B). A431 epidermoid carcinoma cell line responds dissimilarly to EGF concentrations, and while low concentration of EGF induces cell proliferation, higher concentrations result in cell apoptosis. This device generates orthogonal linear gradients of EGFR and MEK inhibitors, and the resultant cell apoptosis gradient in the MCGG demonstrated the ability of the device to determine the combinatorial cell response to specific signaling pathways.¹⁹

1.1.2 Flow-based gradient generators

In the last decade, microfluidic flow-based gradient generators have revolutionized a wide range of chemical and biological practices and produced biochemical concentration gradients for cellular monitoring, and drug screening applications have been one of them.^{1,10,20} MCGGs based on laminar flow can provide desired ranges of biochemical concentration gradients with high precision and controllability by manipulating convective flow.^{12,21} In one study, a microfluidic gradient device was utilized for drug screening and disease modeling with evaluating iPSC-derived motoneurons responses to the riluzole concentration gradient.²² The Microfluidic biochip was constructed with micropillar arrays for trapping uniform-sized neurospheres and promoting neurite network formation. The peripheral channels were connected to the central flow channel through microgrooves that generated a stable concentration gradient with a combination of convection and diffusion. To examine the effect of drug concentration gradient on neurospheres, cells were treated with thapsigargin, a neurotoxin that promotes neuronal death and is a model reagent for neurodegenerative diseases. A concentration gradient of riluzole as a drug to alleviate thapsigargin's neurotoxicity was produced by injecting drugged and drug-free culture

Fig. 1 Design and operation principle of diffusion-based microfluidic orthogonal gradient generators. (A) Static and dynamic versions of the microfluidic gradient generator for producing a combinatorial concentration gradient of morphogens to simulate motor neurons localized differentiation in the process of neural tube development and probing chemotactic response time and adaptation in the tumor microenvironment. (B) A microfluidic device for generating linear orthogonally-aligned gradients of MEK and EGFR inhibitors and analyzing the A431 epidermoid carcinoma cells apoptosis pathway. Panel (A) reproduced with permission from Uzel SG, Amadi OC, Pearl TM, Lee RT, So PT, Kamm RD. Simultaneous or sequential orthogonal gradient formation in a 3D cell culture microfluidic platform. *Small* (Weinheim an der Bergstrasse, Germany). 2016;12(5):612–622. Panel (B) reproduced with permission from Kilinc D, Schwab J, Rampini S, et al. A microfluidic dual gradient generator for conducting cell-based drug combination assays. *Integr. Biol.* 2015;8(1):39–49.

mediums into different inlets. It was shown that riluzole promoted neuro-rescue or neuroprotection in the regions with higher drug concentration, while thapsigargin induced considerable damage to neurospheres in the dead zone.²²

Christmas tree-like gradient generators have been among the most commonly used tools for creating biochemical concentration gradients. In these flow-based microdevices, two reagents with different concentrations combine at repeated T-junctions, and the desired concentration gradient is generated in a direction perpendicular to the fluid flow by diffusion across the laminar flow interface.^{10,23,24} In one study by Tang et al., a bone-on-a-chip microdevice was developed for recapitulating bone tissue microenvironment.²⁵ A hydroxyapatite-PDMS microfluidic concentration gradient chip was fabricated by the stereolithographic printing process, and it contained a ceramic layer and a PDMS cover with Christmas tree-like structure. In high media flow rates, the reagents had inadequate time to diffuse and mix uniformly and could cause excessive shear stress damage to cells, while in low flow rates, there was a lack of sufficient drive to push the fluid forward. To determine the ideal flow rate to generate the appropriate concentration range, a COMSOL flow analysis was applied (Fig. 2A).²⁵ To examine the device's functionality for bone-related drug studies, mouse osteosarcoma cells (UMR-106) were cultured in the device, and a concentration gradient of doxorubicin as a primary antitumor drug for the treatment of osteosarcoma was produced by the Christmas tree gradient generator. The confocal microscopy examinations showed that the number of UMR-106 cells in the region with high drug concentration decreased significantly. Moreover, the DOX concentration in the zone with half of the control group cell population was measured to determine the IC₅₀ of DOX, and the results were validated with the conventional culture plate model.²⁵

Shimizu et al. created an ECM-based MCGG from transglutaminase enzymatically cross-linked gelatin with a porous nature that permitted interstitial flow and generated a culture surface with a controlled biochemical gradient on the surface.²⁶ To evaluate the applicability of the device for drug screening purposes, the response of HUVECs to histamine concentration gradient induced by interstitial flow was examined (Fig. 2B). Endothelial cells have a contracting response to histamine introduction to increase the barrier permeability of the vessel. In this study, the cellular area of the endothelial cells before and after the histamine treatment was measured as the indication of cellular shrinkage, and HUVECs cultured in the high histamine concentration region shrunk significantly greater than the histamine-free region.²⁶

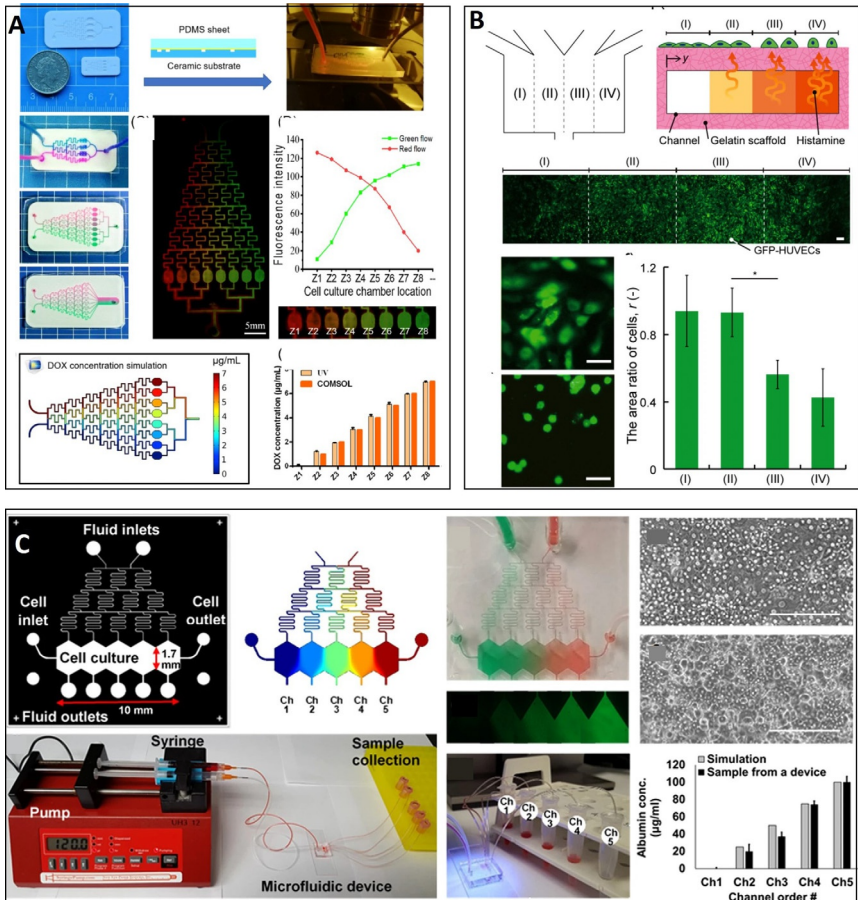


Fig. 2 Design and applications of flow-based microfluidic drug concentration gradient generators. (A) A Christmas tree-like HA-PDMS-based MCGG for creating a concentration gradient of doxorubicin. (B) An ECM-based MCGG for evaluating HUVECs response to histamine concentration. (C) The Metabolic Patterning on a Chip platform for recapitulating liver zonation through concentration gradients of glucagon and insulin to induce the carbohydrate/nitrogen metabolism pattern and examine the drug-induced hepatotoxicity via Cytochrome P450 activity-dependent response to acetaminophen. Panel (A) reproduced from Tang Q, Li X, Lai C, et al. Fabrication of a hydroxyapatite-PDMS microfluidic chip for bone-related cell culture and drug screening. *Bioact. Mater.* 2021;6(1):169–178, under a Creative Commons License. Panel (B) reproduced with permission from Shimizu A, Goh WH, Itai S, Karyappa R, Hashimoto M, Onoe H. ECM-based microfluidic gradient generator for tunable surface environment by interstitial flow. *Biomicrofluidics* 2020;14(4):044106. Panel (C) reproduced from Kang YB, Eo J, Mert S, Yarmush ML, Usta OB. Metabolic patterning on a chip: towards in vitro liver zonation of primary rat and human hepatocytes. *Sci. Rep.* 2018;8(1):8951, under a Creative Common Attribution 4.0 International License.

In another organ-on-chip, a metabolic patterning on a chip (MPOC) was constructed to mimic the liver zonation.²⁷ One key physiological feature of the liver sinusoid is hepatic zonation so that cells display various activities and characteristics based on their location in the liver sinusoid. In this MPOC device, tree-like shape concentration gradients of hormones and enzymatic inducers were produced to create a dynamic metabolic pattern across the cell microchamber and mimic *in vivo*-like liver zonation and zonal toxic response (Fig. 2C).²⁷ The hepatocytes' cell viability and mitochondrial activity gradually decreased across the cell chamber's width from zone 1-like to zone 3-like region due to the higher CYP1A2 activity of the hepatocytes in zone 3.²⁷

1.2 Gradient generators for high-throughput drug screening

In the last years, fast-paced progress in developing microfluidic tools for cell studies and integrating robotics, automated analyzing devices, and biosensors in biomedical microdevices have made the microfluidic biochips promising tools for high-throughput drug screening; therefore, microfluidic platforms like MCGs and microarrays have been the gold standard in drug testing experiments.^{28–32} A microfluidic device was established to cultivate human high-grade glioma cells (UVW) spheroids obtained from human prostate biopsies and test the anticancer drugs by an MCGG tool.³³ In this device, drug solution and culture media were injected into two separate reservoirs on two sides of the cell culture channel to create a symmetrical hydrostatic pressure-driven flow through the cell microarray that concurrently transported drug and media from each side of the channel to the central channels reservoirs (Fig. 3A). This structure produced a self-generated concentration gradient tool for cancer drug screening. UVW spheroids were treated with a concentration gradient of a chemotherapeutic agent called cisplatin, and the cell viability was assessed with PI and FDA double staining. The results showed that the drug concentration was proportional to the spheroid's shape factor parameter, which is a sign of spheroids disaggregation and outline roughness and is a readout for spheroids' health.³³

A disk-like microfluidic gradient generator with compact double spiral mixers was developed in one research for producing three stable, accurate, and controllable drug gradients.³⁴ Two cancer cell lines (MCF-7 and HepG2) were cultured in the device and treated with three different concentration profiles of anticancer drugs (doxorubicin and cisplatin). Doxorubicin, cisplatin, and drug-free medium were injected into the device

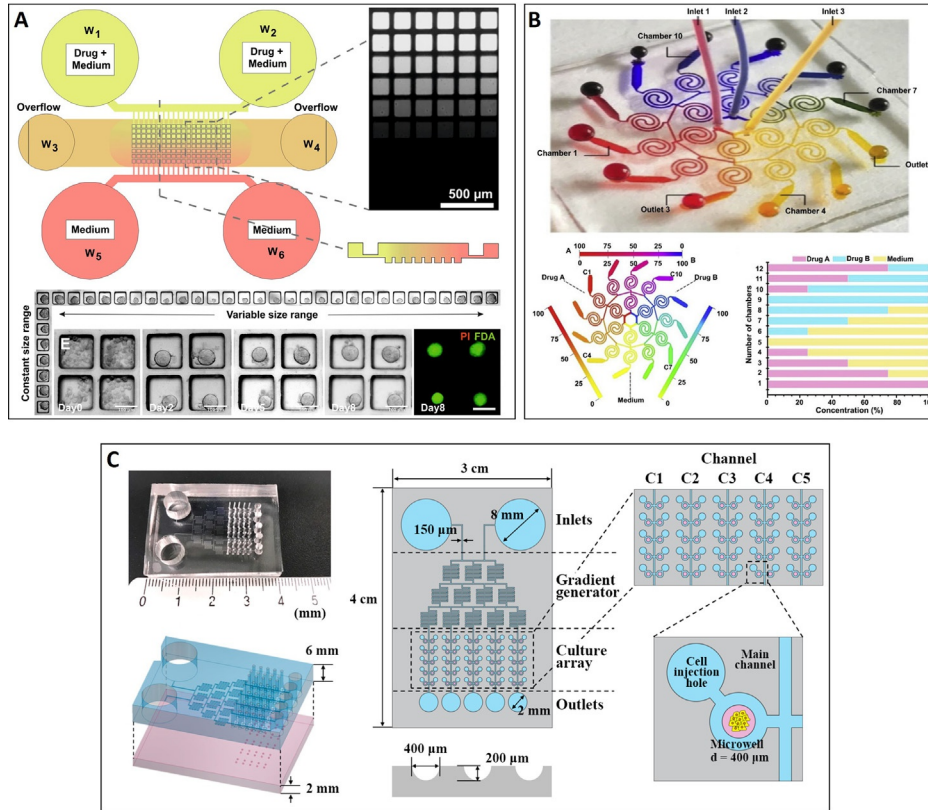


Fig. 3 See figure legend on next page.

via inlet 1,2 and 3, respectively. Consequently, three concentration gradients of doxorubicin, cisplatin, and the combination of the drugs were generated in 12 separate chambers (Fig. 3B). Cells that were cultured in the chambers with high drug concentration for a prolonged time had significantly lower live cell populations, and the most effective concentration profile with the highest cell apoptosis induction was the combination of doxorubicin (75%) and cisplatin (25%) in Chamber 12. The results demonstrated that this device is a powerful tool to generate multidrug concentration gradients for evaluating dose- and time-dependent cell-based studies and high-throughput drug screenings.³⁴

A microfluidic spheroid culture device with a concentration gradient generator was developed for examining cancer drug efficacy (Fig. 3C).³⁵ The colon cancer cell line (HCT116) and glioma cell line (U87) were cultured in the microdevice with concave microwells to form the cancer spheroids with uniform size and distribution. As an anticancer drug, Irinotecan was injected into the chip to produce a concentration gradient, and the functionality of the device was evaluated by monitoring the shape and viability of the cells. Spheroids in the microwells with high irinotecan concentration lost their roundness, collapsed severely, and live/dead staining images indicated that cell viability declined continuously with elevated drug concentration.³⁵

A paper-based microfluidic biochip was constructed to generate a drug concentration gradient and assess cell response to drugs based on high-throughput screening.²⁸ For creating the drug concentration gradient, two solutions containing doxorubicin and buffer were injected in two

Fig. 3 Layout and functions of drug concentration gradient generators for high-throughput drug screening. (A) A microfluidic device for culturing human high-grade glioma cells (UVW) spheroids obtained from human prostate biopsies and producing a self-generated concentration gradient for cancer drug screening. (B) Disc-like microfluidic three concentration gradient generator for analyzing different combinations of doxorubicin and cisplatin on MCF-7 and HepG2 tumor cell lines. (C) A microchip with concave microwells for culturing colon cancer cell line (HCT116) and glioma cell line (U87) spheroids and generating Irinotecan concentration gradient. Panel (A) reproduced from Mulholland T, McAllister M, Patek S, et al. Drug screening of biopsy-derived spheroids using a self-generated microfluidic concentration gradient. *Sci. Rep.* 2018;8(1):14672, under a Creative Common Attribution 4.0 International License. Panel (B) reproduced with permission from Shen S, Zhang X, Zhang F, Wang D, Long D, Niu Y. Three-gradient constructions in a flow-rate insensitive microfluidic system for drug screening towards personalized treatment. *Talanta* 2020;208:120477. Panel (C) reproduce from Lim W, Park S. A microfluidic spheroid culture device with a concentration gradient generator for high-throughput screening of drug efficacy. *Molecules* 2018;23(12):3355, under an open access Creative Common CC BY license.

separate inlets, and HeLa cells encapsulated in the collagen type I matrix were cultured in a microwells array, and a contrary trend of cell viability compared with drug concentration was shown. In paper-based micro-devices, fluid flow is mainly derived by capillary force in porous paper channels, and there is no need for additional equipment like pumps and valves. Moreover, in flow-based MCGGs, operating the device for a prolonged time would be quite costly due to the excessive reagent requirement, while in paper-based tools, the solution consumption is significantly reduced.²⁸

1.3 Challenges and possible solutions for microfluidic drug delivery at cellular level

Although various microfluidic platforms have been developed so far for recapitulating drug–cell interactions and mimic *in vivo* cellular microenvironment of different tissues, there are still some limitations in the micro-physiological complexity and drug-induced cellular pathways resemblance.¹¹ Microfluidic systems for dynamic fluid manipulation and cell culture have revolutionized the research in concentration gradient generators by introducing state-of-the-art designs and configurations with extraordinary precision in flow control geometric constraints to form gradients with high stability and accuracy. These systems, based on the type of the microdevice, could rely on only molecular diffusion or diffusion-convection phenomena for generating gradients.^{1,12}

Diffusion-based MCGGs compared to flow-based platforms, have a more cost-effective setup, are needless of expensive pumping systems, and minimize the cell damage due to a shear stress-free environment. However, these flow-free gradient generators are commonly much slower in producing the concentration gradient and require improvements in gradient stability and significant reduction of source-sink replenishment frequency.^{1,12,18} Convection-based tools are able to sustain a drug concentration gradient within a fluid-flow environment and are suitable for the maintenance of a biochemical gradient within a specific tissue.²¹ Moreover, these flow-based systems can create concentration gradients rapidly in a small area because of their short relaxation time and large Péclet (Pe) number, making them appropriate for applications where quick response is required. Though the significant hurdle in these devices is that, the gradient at a fast flow rate can damage the cells and ultimately trigger adverse efficiency in the cell signaling system.^{19,20} To alleviate the problem, one recommended solution has been applying interconnected microgrooves and separate chambers for minimizing the effect of shear stress and generating long-term stable concentration gradients.²²

In traditional tree-like microdevices, cells cultivated on the surface of the microchambers are exposed to direct biochemical factors from the fluid flow. In contrast, in the physiological microenvironment, cells are exposed to a complex and controlled concentration gradient of soluble factors through an interstitial flow.²⁶ Biomimetic hydrogels like collagen and agarose can increase the system's physiological relevance, generate a 3D scaffold environment for embedded cells, and recapitulate *in vivo*-like concentration gradients. These 3D ECM-like constructs could mimic tissue physiological functions such as microvasculature formation and axon guidance by chemotaxis due to their porous nature, albeit hydrogel-based systems usually are limited in throughput and spatiotemporal gradient conditions due to slow diffusion rate and also add experimental complexity and variability to the system.^{15,16,18,32} The gradient in most common MCGGs is limited to one or multiple fixed perpendicular directions that restrict the positioning and orientation of drug gradients for cell re-orientation and migration assays. An omnidirectional radially symmetric MCGG was developed to overcome this concern for orienting laminar flow in 360° freely and manipulating chemical profiles in time and space.³⁶

There is currently an urgent need to execute accurate and high-throughput predictive *in vitro* platforms in the pharmaceutical industry that resembles human biology like biochemical concentration gradients at a higher level and cut the time-consuming and costly drug procedures discovery pipeline.^{11,28,30} Microfluidic systems have displayed remarkable benefits for drug screening assays due to their capacity for miniaturization and parallelization. Repeatable and robust results could be generated for an extended period with a high level of organotypicalness and *in vivo* microenvironment resemblance by employing scaled-down biosensors and automated features. The balance between the operational simplicity and biological complexity may end up with the commercialization of MCGGs and improve the user-friendliness of these microdevices.^{11,29,32}



2. Microfluidic *in vitro* drug delivery at tissue level

There is an urgent necessity in the drug screening development pipeline for emerging predictive laboratory tissue models that truly orchestrate *in vivo* microenvironment and drug-cell interactions.^{37,38} Conventional 2D or 3D *in vitro* platforms lack physiologically-relevant tissue microstructure, sustained cell viability, functional stability, and unchanged cellular morphology and phenotype.^{39,40} In the past years, microfluidic tissue on

chips have transformed the study of complex biologic practices like drug metabolism/toxicity and cancer research, and with monitoring spatiotemporal factors, these microdevices are capable of recapitulating the *in vivo*-like microenvironment properties like cell–cell and cell–ECM interactions, cellular composition, and tissue 3D microarchitecture.^{2–4,41}

Novel patient-specific drug-testing tools are needed in cancer research and personalized medicine due to the current oncology drug development pipeline.^{41,42} In one research, microdissected tissues (MDT) were obtained from live tumor tissue and were segmented reproducibly to submillimeter sections and cultured on an MDT-on-chip (Fig. 4A). The objective was to obtain tissue sections large enough to resemble biologically relevant gradients of nutrients, waste, and signaling molecules while also being small enough to preserve high viability all over the tissue without oxygen deficiency in the center. The microfluidic platform was able to trap the microtissues in a low shear stress environment, and the chemosensitivity of patient-derived ovarian cancer MDTs to carboplatin was evaluated by loading the drug into the microchannels and measuring the chemoresponse of treated and nontreated cell populations.⁴¹

In a study by Yin et al., a Microfluidic Kidney Chip was constructed for coculturing renal proximal tubular epithelial cells (RPTECs) and peritubular capillary endothelial cells (PCECs) and nephrotoxicity assessment.⁴³ The kidney-on-chip consisted of three parts: drug concentration gradient generator, three-layer microfluidic organ chip, and flow-temperature control device (Fig. 4B). The two groups of drug concentrations were produced on the gradient chip, then RPTECs and PCECs were seeded on opposite sides of membranes, and after the drug treatment, RPTECs' viability was evaluated to determine the influence of that drug. Finally, a flow-temperature control device was activated to stabilize the environments for prolonged cell culture. The results demonstrated a significant reduction in cisplatin-induced nephrotoxicity caused by the intervention of cimetidine in the microchip. This controllable biomimetic kidney model replicated critical aspects of kidney biological features, drug response, resistance, and toxicity could speed up the drug discovery and screening practices.⁴³

In the drug delivery at the cellular level section, we described the MCGGs for drug delivery and toxicity testing; however, these platforms can generate concentration gradients in a micron-sized level (e.g., cells).^{20,28,44} Therefore, there is a dire need to introduce an MCGG that can produce continuous concentration gradients of multi mixtures (e.g., drugs) in a millimeter-sized sample (e.g., tissue, spheroids). Rismanian et al. proposed a new class of MCGG

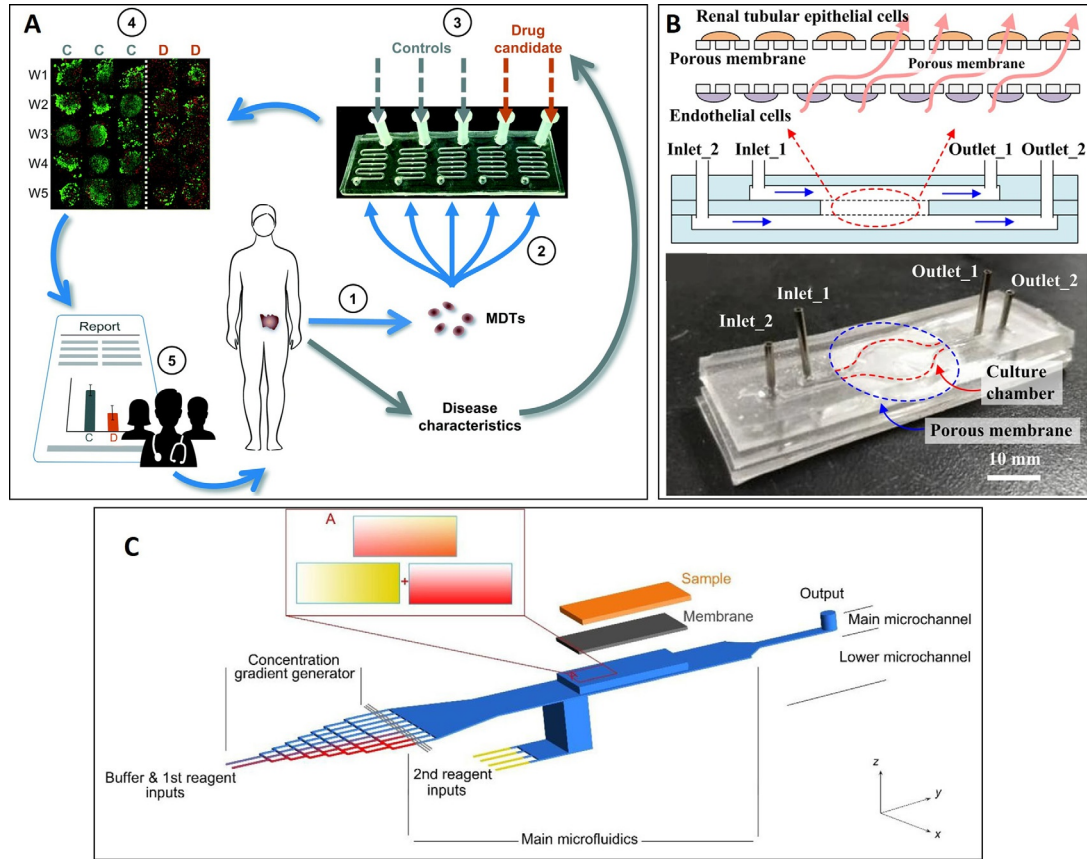


Fig. 4 See figure legend on opposite page.

by linking a modified tree-like CGG with a micromixer to develop a so-called Millimeter-sized sample /Multireagents/ Continuous CG with a diffusion-convection-based approach (Fig. 4C).²⁰ This microdevice introduced two reagents concurrently with a continuous concentration gradient of two inlets to deliver the reagents to a millimeter-sized sample (e.g., microtissue). This microchip with measurable concentration relaxation time and low effect of variability in the sample's porosity and permeability and diffusivity of various drugs could be an ideal tool for *ex vivo* drug chemosensitivity testing in personalized medicine.²⁰

The high complexity and heterogeneity of the tumor microenvironment play a substantial part in drug resistance and chemoresponse.^{45–47} Moreover, the endothelium is essential in systemic drug delivery, provides nutrients and oxygen to the tumor, and plays a crucial role in promoting new blood vessel formation *via* angiogenesis. Thus, a simple capillary force-based microchip for 3D tumor tissue–2D endothelium interfaces and drug testing was developed in a study. In this work, breast tumor cells were cultured in 3D micro-wells, and the endothelial barrier was modeled on top of the 3D culture by seeding HUVEC cells as an endothelium.⁴⁷ The endothelium was efficient and displayed physiological features, like the preferential proliferation of cells with higher access to nutrients and oxygen. Next, the drug penetration and toxicity assays were conducted in the tumor–endothelium model, and death ligand TRAIL (TNF-related apoptosis-inducing ligand) conjugates with a sizeable unilamellar vesicle (LUV) was tested. The results demonstrated that LUV-TRAIL prompted cell death in a higher number and was more effective than TRAIL.⁴⁷

Fig. 4 Microfluidic systems for drug delivery and assessment at the tissue level. (A) Microdissected Tumor on-chip for *ex vivo* drug testing and personalized medicine. (B) A Microfluidic Kidney Chip for coculturing kidney cells and efficient drug screening and cisplatin-induced nephrotoxicity assessment. (C) A Millimeter sized sample/multireagents/continuous concentration generator with functionality in drug chemosensitivity testing for personalized medicine. Panel (A) reproduced with permission from Astolfi M, Péant B, Lateef MA, et al. Micro-dissected tumor tissues on chip: an *ex vivo* method for drug testing and personalized therapy. *Lab Chip* 2016;16(2):312–325. Panel (B) reproduced from Yin L, Du G, Zhang B, et al. Efficient drug screening and nephrotoxicity assessment on co-culture microfluidic kidney chip. *Sci. Rep.* 2020;10(1):6568, under a Creative Common Attribution 4.0 International License. Panel (C) reproduced with permission from Rismanian M, Saidi MS, Kashaninejad N. A microfluidic concentration gradient generator for simultaneous delivery of two reagents on a millimeter-sized sample. *J. Flow Chem.* 2020;10:615–625.

According to the reports analyzing different compounds' clinical developments, oncology drug development's success rate from phase 1, clinical trials to FDA approval is less than 4%.⁴⁸ This low success rate in clinical trials demonstrates the deficiencies in existing prescreening methods. In another study, a Tumor Chip system was introduced to deliver cancer–stromal interaction, dynamic perfusion, replicate microvasculature, and high-throughput, as shown in Fig. 5A.⁴⁹ The L-TumorChip was a three-layered biochip with spatial control over the reconstruction of microvessels and tumor compartments, with continuous media perfusion. The tumor compartment consisted of human microvascular endothelial cells (HMVEC) and Matrigel-encapsulated breast cancer cells culture layers, separated by a thin membrane to mimic the *in vivo* tumor microenvironment. The tumor biochip was capable of real-time drug response monitoring for high-throughput drug kinetics studies. The drug responses to doxorubicin treatment showed that the presence of cancer-associated fibroblasts affects drug pharmacokinetics, while apoptotic reactions specified by caspase-3 activities are higher in the coculture of cancer cells with normal fibroblasts.⁴⁹

In another research, a chip-based breast cancer equivalent with a tumor-replicating microvasculature was developed to recapitulate the breast tumors' physiology and pathophysiology and assess anticancer drug effectiveness.⁵⁰ For resembling high and low flow perfusion regions in the tumor microenvironment, two specific microvascular designs from mouse vascular networks were applied for tumor-mimetic chip production. The two regions with different degrees of fluidic exchange between the microvascular channels and the central tumor chamber represent well-perfused and poorly-perfused breast tumors. Breast cancer cells were cocultured for a prolonged time in 3D hydrogel-based structure with stromal fibroblasts, and the interstitial space between the chambers and endothelium with porous vasculature mimicked the physiological cancer-endothelial cell interactions. Before activating their cytotoxic activity, anticancer drugs must overcome particular rate-controlling steps like the ability to perfuse through the microvasculature and transport to the site of interest. In this work, doxorubicin and paclitaxel were introduced to the breast tumor-on-chip, and the cell viability was assessed. A remarkable reduction in viable tumor areas was observed across all tested conditions, specifically in high perfusion chips, because of higher drug penetration levels in the central tumor chambers.⁵⁰

Glioblastoma multiforme (GBM), an extremely aggressive and high-grade type of brain cancer, has a poor prognosis, with an average survival time of 12–18 months—only 25% of glioblastoma patients survive more

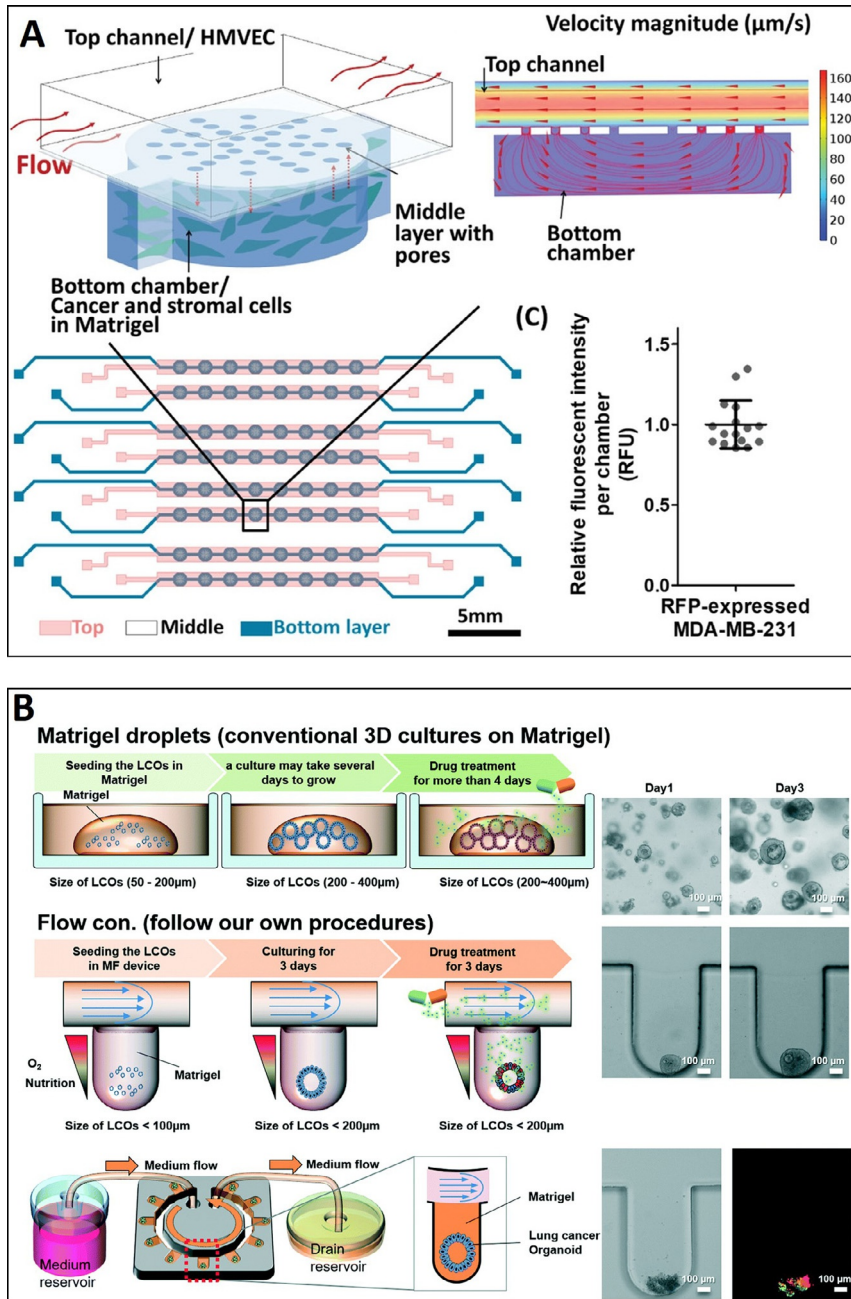


Fig. 5 Chip-based platforms for investigating tumor microenvironment and drug pharmacokinetics. (A) A high-throughput tumor-on-a-chip platform for emulating certain tumor-stroma and tumor–endothelium interactions and the stromal effects on drug

(Continued)

than 1 year, and only 5% of patients survive more than 5 years—with standard GBM therapies.^{51,52} To address this concern, a brain cancer chip for assessing tumor cell drug responses was administered to analyze drugs more efficiently in preclinical trials and improve patient survival.⁵³ In this work, 3D spheroids obtained from three patient GBM tumor cells were cultured on a hydrogel layer with a concentration gradient generating design to produce two drug concentrations (FDA-approved temozolomide and bevacizumab) simultaneously. The result of drug analysis indicated a common tendency toward higher cytotoxicity of two drugs combined with single-drug treatment and a more robust efficacy of temozolomide than bevacizumab.⁵³

Colorectal cancer is now the third major cause of cancer-related death in women and the second in men, primarily due to the high rate of cancer metastasis and chemotherapeutic treatment ineffectiveness.^{54,55} There is a dire need for more reliable and predictable screening approaches for colorectal cancer drug development. In one research, a biomimetic tumor-on-a-chip platform was developed to emulate *in vivo* relevant colorectal tumor microenvironment and reconstruct functional microvasculature for precision nanomedicine delivery.⁵⁶ Colorectal cancer cells were seeded in matrigel-supported 3D structure, while endothelial cells were cultured in a 3D vessel like architecture. To examine the concentration-dependent response of cells inside the biochip to the antitumor drug, gemcitabine (GEM) was loaded in CMChT/PAMAM dendrimer nanoparticles for delivering the drug to HCT-116 cancer cell line. With introducing GEM-loaded dendrimer nanoparticles to the microchannels, cell death occurred in a gradient manner, which demonstrated that GEM could be efficiently released from the nanoparticles and taken up by the CRCs as a useful anticancer therapeutic.⁵⁶

As a preclinical method, tumor organoids are advantageous for patient-specific treatment thanks to their ability to sustain critical biological tissues' physiological and structural features.^{57,58} Jung et al. developed a microfluidic-based 3D lung cancer organoid culture platform enabling drug

Fig. 5—Cont'd responses to doxorubicin treatment. (B) Microfluidic biochip for three-dimensional lung cancer organoid culturing and cisplatin and etoposide apoptosis tests. *Panel (A) reproduced with permission from Chi C-W, Lao Y-H, Ahmed AHR, et al. 2020 High-throughput tumor-on-a-chip platform to study tumor–stroma interactions and drug pharmacokinetics. Adv. Healthc. Mater. n/a(n/a):2000880. Panel (B) reproduced with permission from Jung DJ, Shin TH, Kim M, Sung CO, Jang SJ, Jeong GS. A one-stop microfluidic-based lung cancer organoid culture platform for testing drug sensitivity. Lab Chip 2019;19(17):2854–2865.*

sensitivity tests directly on a microphysiological system, as shown in Fig. 5B.⁵⁹ This platform had high control over the size of lung cancer organoids (LCO) and validated the production of LCOs derived from primary small-cell lung cancer tumors with rapid proliferation and exhibition of disease-specific characteristics. The first-line chemotherapeutic for Lung cancer (cisplatin and etoposide) was chosen as the test drugs in this work. While the LCO cores and cells located away from blood vessels were more resistant to chemotherapy and remained viable, apoptosis was shown in cells around the organoid outer region. The drug concentration was associated with reduced rates of cell viability.⁵⁹

Hepatocellular carcinoma has become the second major cause of cancer-related death, with an occurrence rate of about 850,000 new patients each year. As a result of 2D cell culture models' incapability in mimicking complex liver pathophysiology and predicting the toxicity of the compounds, few new anticancer drugs are available now.^{60,61} In one research, a biomimetic 3D liver cancer-on-chip was developed, and decellularized liver matrix (DLM) was obtained from rat liver tissue to integrate the ECM proteins and GelMa into the liver chip.⁶¹ This system had an improved competence to maintain hepatocytes viability and functions under perfusion conditions and may be accredited to establish biochemical factors, the maintenance of scaffold proteins, and the restoration of biophysical and biomechanical cues enhanced resemblance of the 3D liver tumor microenvironment. For assessing the platform's drug analyzing capability, acetaminophen and sorafenib were tested for dose-dependent drug toxicity, and linear dose-dependent hepatotoxicity was detected for both drugs in terms of HepG2 cells viability, urea secretion, and albumin production.⁶¹



3. Microfluidic *in situ* drug delivery at organ level

Recent advances in microfabrication technology revolutionized the drug delivery system. Microneedle (MN) is a noninvasive and painless localized drug delivery system (DDS) that prevents gastrointestinal degradation and bypasses hepatic metabolism. MNs have been used for drug delivery to different organs, including skin, oral mucosa, vaginal mucosa, ocular tissue, nail, anal sphincter, dermal papilla, and cardiac muscle.^{62–65} Fig. 6A and B demonstrate the MNs DDS used for a drug-eluting balloon of vascular tissue⁶⁶ and intra-corneal drug injection,⁶⁷ respectively. Various drugs such as insulin,^{68,69} calcein,⁶⁹ DNA vaccine and nucleic acids,⁶⁹ nanomedicine,^{69,70} ocular and chronic wounds treated drug,^{69,71} peptide or subunit vaccination, and cancer therapeutics⁷² have been delivered by MN drug delivery system. MNs are

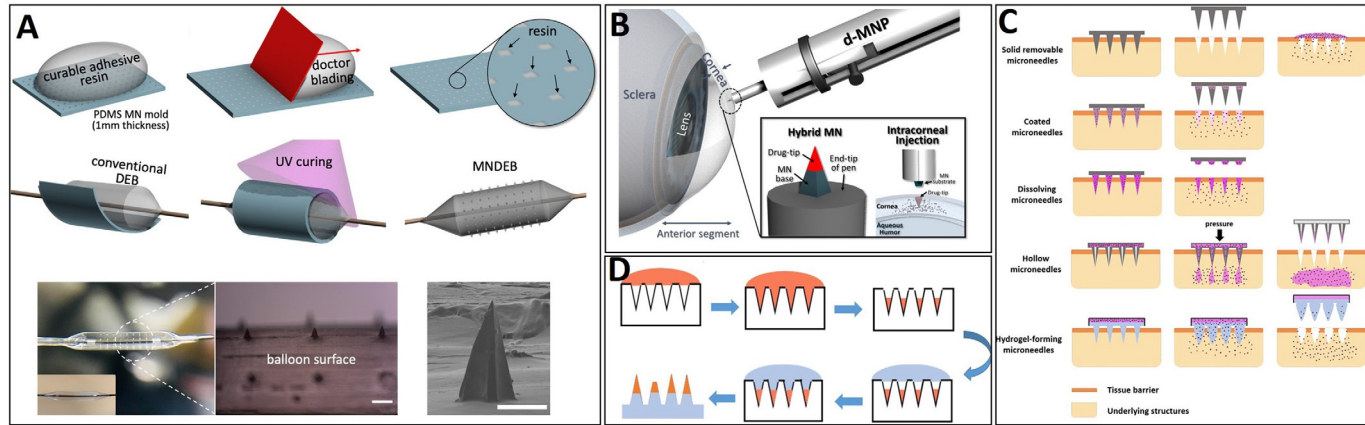


Fig. 6 See figure legend on opposite page.

structures of the arrowhead, bullet, conical, cylindrical, pyramidal, obelisk, octagonal cone shape with the height average between super-short ($<100\text{ }\mu\text{m}$) to super-long ($>1000\text{ }\mu\text{m}$), the width of $50\text{--}250\text{ }\mu\text{m}$, and the tip thickness of $1\text{--}25\text{ }\mu\text{m}$.^{73–75} Both sizes and shapes of MNs affect the mechanical strength of the MN and the skin penetration's depth.⁷⁶ MNs have been fabricated through various microfabrication techniques such as casting, dry etching, wet etching, micromolding, 3D-printing, electroplating, laser ablation, magnetorheological, and drawing lithography.^{75,77} The most-reported microfabrication technique for MNs is the casting method, a low-cost, massproductive, and easy to operation method shown in Fig. 6D. Depending on their applications, MNs are made from different materials, including silicone, metals, polymers,⁷⁸ and ceramics.⁷⁹ The material that is used for MN fabrication must be safe, nontoxic, and strong enough to penetrate the skin.^{80,81} Based on the drug delivery route, MNs can be categorized

Fig. 6 MNs DDS. (A) MNs integrated with eluting balloon for drug delivery to vascular tissue, (a–c) conformal transfer molding steps consisting of premolding with UV curable adhesive resin, (d) alignment the drug eluting balloons (DEB) with flexible planar PDMS mold, (e) UV curing process and (f) completed MNDEB, (g) Stereo- and optical microscopic images of MNDEB and MNs MN onto MNDEB surface (scale bar = $300\text{ }\mu\text{m}$) (h) the scanning electron microscopic image of the constructed MN in the MNDEB surface, (scale bar = $100\text{ }\mu\text{m}$). (B) Schematic of sustained drug releasing system using a detachable hybrid microneedle pen system for intracorneal drug injection. (C) Schematic representation of the MNs DDS with five different drug delivery mechanisms, (a) Solid MNs that are used as puncher to create micropores in the skin to increase the permeability, (b) Coated MNs that contain drug on the surface which released after penetration, (c) Dissolvable MNs that released the drug due to dissolution once inserted into the tissue, (d) Hollow MNs that injected the drug into the tissue from the external reservoir by pressure-driven flow or diffusion mechanism. (e) Swollen MNs that absorb the ISF after insertion and administrate the drug. (D) The casting fabrication process of two layers MNs consists of 2 components. (a) pouring component 1 into the mold, (b) vacuumed or centrifuged to release air bubbles, (c) solidification component 1, (d) pouring component 2 as the second layer, (e) vacuumed or centrifuged, (f) Peeled away solidified two-layer MNs. Panel (A) reproduced with permission from Lee K, Lee J, Lee SG, et al. *Microneedle drug eluting balloon for enhanced drug delivery to vascular tissue*. J. Control. Release. 2020;321:174–183. Panel (B) reproduced with permission from Lee K, Song HB, Cho W, Kim JH, Kim JH, Ryu W. *Intracorneal injection of a detachable hybrid microneedle for sustained drug delivery*. Acta Biomater. 2018;80:48–57. Panel (C) reproduced with some changes from Rzhevskiy AS, Singh TRR, Donnelly RF, Anissimov YG. *Microneedles as the technique of drug delivery enhancement in diverse organs and tissues*. J. Control. Release. 2018;270:184–202. Panel (D) reproduce with permission from Zhuang J, Rao F, Wu D, et al. *Study on the fabrication and characterization of tip-loaded dissolving microneedles for transdermal drug delivery*. Eur. J. Pharm. Biopharm. 2020;157:66–73.

into five groups that are solid MN, coated MNs, hollow MN, dissolvable MNs, and swollen MNs that are shown in Fig. 6C. In the following, each group will be discussed in more detail to address the operation mechanism, material, fabrication method, and challenges.

3.1 Solid microneedles

The first generation of MNs is solid MNs. Solid MNs were applied as micro punchers to produce small pores in the skin and increase skin penetration. After solid MN insertion, the drug in the form of liquid, cream, gel, or lotion is applied in created pores, as shown in Fig. 6C(a). Different types of materials, including silicone, metals (stainless steel, titanium), polymers,⁷⁸ and ceramics,⁷⁹ have been used for solid MNs preparation. Solid MNs have been fabricated through various techniques such as dry etching, wet etching, micro-molding, 3D-printing, electroplating, laser ablation, magnet-orheological, and drawing lithography.⁸² Various drug formulations such as Nicardipine HCl, Amantadine HCl, Tiagabine HCl, Pramipexole, dihydrochloride, and Carbamazepine have been administered *via* solid MNs.⁸³ Solid MNs can be made from a wide range of materials that are an excellent factor for accessibility. However, solid MNs fracture under the skin is a challenging task. There also some concerns regarding the two-step drug delivery using solid MNs that increase the odds of contamination.

3.2 Coated microneedles

Coated MNs are generally solid MNs that are coated with matrix drug loaded. After MNs insertion into the skin, the coating layer will be dissolved, and the drug will be released, Fig. 6C(b). This group of MNs was made from metal, silicon, and nondegradable polymers that were coated with biomaterial matrices such as carboxymethyl cellulose sodium salt, hyaluronic acid, methylcellulose, polyvinyl alcohol, polyvinyl pyrrolidone, polylactic acid, polycaprolactone, sucrose, and (2-hydroxypropyl)- β -cyclodextrin.⁷³ The key parameters of the coated material are hydrophilicity, biocompatibility, and biodegradability. Some stabilizers were usually added to the matrix to decrease the damage to the therapeutics, such as dextran, glucose, inulin, sucrose, and trehalose.⁷³ There are various coating methods such as dip coating, gas-jet drying, rolling coating, spray coating, electrohydrodynamic atomization coating, and layer-by-layer coating.^{73,84} The biggest drawback of the coated MNs is the low drug loading capacity because, in such type of MN, a very small dose of drug material is only coated on the surface of the

MN. For example, for polylactic acid MNs that were coated with a solution of sulforhodamine B, the drug loadings were up to 18 ng per needle for 750 μm MNs. It was shown that by increasing the viscosity of the coating solutions, the drug loading could be increased. However, the drug delivery efficiency was reported as 90%.⁸⁵

3.3 Dissolvable microneedles

Dissolvable MNs are made from dissolvable material in aqueous media. After insertion, MNs absorb the interstitial fluid (ISF) and eventually dissolve, leading to the sequential release of the loaded drug, Fig. 6C(c). Dissolvable MNs can be made from a quick or long-time dissolvable material, making them good candidates for controlled-release delivery.^{86–88} Biopolymers and sugars material similar to coated MNs were commonly used to prepare dissolvable MNs through micromolding,⁷⁵ casting,⁸⁹ drawing lithography, droplet-born air blowing methods.⁹⁰ As a significant advantage, there is no limitation for the size of therapeutic molecules for applying in dissolvable MNs. Similar to the coated MNs, the efficiency of drug delivery of the dissolved MNs depends on the dissolution of the matrix. However, the agent dosing is much higher for dissolved MNs. This group of MNs is economical and effective, thus attracting many researchers' attention, and promising good tools for MNs DDS.^{88,91,92} One of the major problems with the dissolvable MNs were poor mechanical strength and weakness to penetrate the skin, however, recently acceptable strong MNs were reported.^{93–96} For example, dissolvable polymeric MNs with a small amount of graphene oxide (GO) was used for the transdermal delivery of the chemotherapeutic, HA15, to melanoma-bearing mouse models. MNs demonstrated good mechanical strength (10–17 times at 500 mg/mL GO), increased moisture resistance, self-sterilization, antibacterial and anti-inflammatory properties, and controlled drug release by near-infrared light-activated.⁹⁴ There are two categories of dissolvable MNs, hole body and tip loaded systems. In the first category, the hole MN body was made of dissolvable material, while in the second one, only the tip of the MNs consists of dissolvable drug-loaded material.^{67,97,98} An MN with a drug-loaded biodegradable tip and a supporting base was developed to sustain drug release into the cornea of an *Acanthamoeba* keratitis mouse model. Follow-up administration for 7 days confirmed the therapeutic efficacy of tip-loaded MN.⁶⁷ Although the tip-loaded MNs facilitate drug penetration into the deeper region, the dose of the loaded drug is small as the small volume tip.

3.4 Hollow microneedles

Hollow MNs are a miniature version of hypodermic needles. After hollow MNs insertion, the drug is injected under the tissue by pressure-driven flow or diffusion, Fig. 6C(d). Agent dosing is more for hollow MNs in comparison with the other kind of MNs. For example, a single hollow microneedle was integrated with a magnetic polymer composites device and inductive sensing instrument to controlled drug release as a wireless pumping system. The fabricated system was able to dosage sensing.⁹⁹ Hollow MNs were made in various configurations with out-off-center pore and side hole. They have been mainly prepared from similar materials for solid MNs, such as silicon metals, glass, polymers,⁸¹ using the multistep process of deep reactive ion etching, wet chemical etching, plasma etching, isotropic etching, laser micromachining, digital light processing-based projection stereolithography, micropipette pulling, and sacrificial micromolding.⁷⁹ Due to the complex geometry of the hollow MNs, the manufacturing process of this type of MNs are more complicated and time-consuming than the others.

3.5 Swollen microneedles

A new generation of the MNs is swollen MNs fabricated from swollen materials such as hydrogels. After the insertion, the MNs will swell due to ISF absorption and subsequently, the loaded agent released, Fig. 6C(e). Swollen MNs were prepared from the combination of the swollen polymers such as methyl vinyl ether and maleic anhydride (PMVE/MAH) and polyethyleneglycol (PEG), PMVE and maleic acid and PEG, 2-hydroxyethyl methacrylate and ethylene glycol dimethacrylate, polyvinyl alcohol, ethyl acrylate, and methacrylate.^{73,100} The most common fabrication method of the swollen MNs is the casting method. For example, silk fibroin scaffold was used with poly(ethylene glycol) diacrylate and sucrose as the needle matrix to fabricate swollen MNs with three formulations of drugs, including Rhodamine B, doxorubicin, and indocyanine green.¹⁰¹ Like hollow MNs, swollen MNs create conduct for drug delivery that can continuously insert the agent from the external reservoir. However, the administration time for the swollen MNs is greater than hollow MNs, which makes the drug delivery time-consuming.

3.6 Challenge of microneedle drug delivery systems

MNs drug delivery has many benefits: MNs realize noninvasive drug delivery, have better patient compliance because of reducing dose frequency,

realize the possibility of self-administration, prevent first-pass metabolism and gastrointestinal incompatibility, have minimal or no side effects, can maintain the plasma drug level, have the possibility of large molecules administration, and are suitable for the drug with short biological half-life and narrow therapeutic index.¹⁰² However, there are some limitations and challenges for using MNs for drug delivery, including less accuracy of dose compared to conventional hypodermic needles, variation in delivery due to skin condition, skin-dependent penetration mechanism, the possibility of tissue damage and venous collapse due to repetitive injection, and risk of breaking and remaining under the skin in case of using nonbiodegradable MNs.¹⁰³



4. Conclusion and future perspective

Miniaturization offers significant advantages in drug delivery application that can be realized using microfluidic technology. In this chapter, the focus was given to *in vitro* and *in situ* microfluidic systems for drug delivery. To this aim, first, the latest advances in developing microfluidic concentration gradient generators (MCGGs) that can deliver the drug at cellular level were discussed. In particular, both diffusion-based and flow-based MCGGs as well as gradient generators for high-throughput drug screening, were thoroughly evaluated. These systems have become an essential tool for studying biological phenomena like cell migration, proliferation, chemotaxis, drug screening, and personalized medicine. Next, we evaluated the state-of-the-art lab-on-a-chip systems for *in vitro* drug delivery at tissue level was investigated. Finally, the design and fabrication of various *in situ* microneedle-based drug delivery systems, including solid microneedles, coated microneedles, hollow microneedles, microneedles dissolvable and swollen microneedles, were explained. We concluded each part by briefly identifying the present challenges and presenting the possible solutions.

Although tremendous efforts have been made in the design, fabrication and characterization of microfluidic devices for drug delivery applications, this field, especially *in vivo* microfluidic drug delivery platforms, is still at a preliminary stage. There are still many challenges that need be addressed in order to realize an efficient implantable microfluidic device for controlled drug delivery. Besides biocompatibility and biodegradability, one of the major challenges of the *in vivo* microfluidic systems for drug delivery is the integration of an efficient mechanism for continuous pumping the drug or the therapeutic agent in the body. It should be done autonomously using

mainly through capillary action or other self-powered microfluidic pump.¹⁰⁴ Efficient integration of such a self-powered microfluidic pump with microneedles can open up a great avenue in this field, leading to revolutionary drug delivery and vaccine administration platforms. Moreover, droplet-based microfluidics,¹⁰⁵ flow-focusing droplet generators¹⁰⁶ and magnetofluidics¹⁰⁷ are other highly efficient platforms that can potentially be used for both drug synthesis and controlled delivery. There are still plenty of rooms in improving such platforms for *in vivo* drug delivery and personalized medicine.

References

1. Nguyen N-T, Shaegh SAM, Kashaninejad N, Phan D-T. Design, fabrication and characterization of drug delivery systems based on lab-on-a-chip technology. *Adv Drug Deliv Rev.* 2013;65(11):1403–1419.
2. Bhatia SN, Ingber DE. Microfluidic organs-on-chips. *Nat Biotechnol.* 2014;32:760.
3. Esch EW, Bahinski A, Huh D. Organs-on-chips at the frontiers of drug discovery. *Nat Rev Drug Discov.* 2015;14(4):248–260.
4. Zhang B, Korolj A, Lai BFL, Radisic M. Advances in organ-on-a-chip engineering. *Nat Rev Mater.* 2018;3(8):257–278.
5. Shintu L, Baudoin R, Navratil V, et al. Metabolomics-on-a-chip and predictive systems toxicology in microfluidic bioartificial organs. *Anal Chem.* 2012;84(4):1840–1848.
6. Haddrick M, Simpson PB. Organ-on-a-chip technology: turning its potential for clinical benefit into reality. *Drug Discov Today.* 2019;24(5):1217–1223.
7. Kashaninejad N, Chan WK, Nguyen N-T. Fluid mechanics of flow through rectangular hydrophobic microchannels. In: *Paper Presented at: International Conference on Nanochannels, Microchannels, and Minichannels*; 2011.
8. Wu Q, Liu J, Wang X, et al. Organ-on-a-chip: recent breakthroughs and future prospects. *Biomed Eng Online.* 2020;19(1):9.
9. Lin JM. *Cell Analysis on Microfluidics*. Singapore: Springer; 2017.
10. Rismanian M, Saidi MS, Kashaninejad N. A new non-dimensional parameter to obtain the minimum mixing length in tree-like concentration gradient generators. *Chem Eng Sci.* 2019;195:120–126.
11. Moradi E, Jalili-Firoozinezhad S, Solati-Hashjin M. Microfluidic organ-on-a-chip models of human liver tissue. *Acta Biomater.* 2020;116:67–83.
12. Dravid A, Raos B, Aqrawe Z, Parittotokkaporn S, O'Carroll SJ, Svirskis D. A macroscopic diffusion-based gradient generator to establish concentration gradients of soluble molecules within hydrogel scaffolds for cell culture. *Front Chem.* 2019;7:638.
13. Shi H, Nie K, Dong B, Long M, Xu H, Liu Z. Recent progress of microfluidic reactors for biomedical applications. *Chem Eng J.* 2019;361:635–650.
14. Cabaleiro JM. Flowrate independent 3D printed microfluidic concentration gradient generator. *Chem Eng J.* 2020;382:122742.
15. Ahrens L, Tanaka S, Vonwil D, Christensen J, Iber D, Shastri VP. Generation of 3D soluble signal gradients in cell-laden hydrogels using passive diffusion. *Adv Biosyst.* 2019;3(1):1800237.
16. Barata D, Spennati G, Correia C, et al. Development of a shear stress-free microfluidic gradient generator capable of quantitatively analyzing single-cell morphology. *Biomed Microdevices.* 2017;19(4):81.

17. Jin T, Xu X, Hereld D. Chemotaxis, chemokine receptors and human disease. *Cytokine*. 2008;44(1):1–8.
18. Uzel SG, Amadi OC, Pearl TM, Lee RT, So PT, Kamm RD. Simultaneous or sequential orthogonal gradient formation in a 3D cell culture microfluidic platform. *Small (Weinheim an der Bergstrasse, Germany)*. 2016;12(5):612–622.
19. Kilinc D, Schwab J, Rampini S, et al. A microfluidic dual gradient generator for conducting cell-based drug combination assays. *Integr Biol*. 2015;8(1):39–49.
20. Rismanian M, Saidi MS, Kashaninejad N. A microfluidic concentration gradient generator for simultaneous delivery of two reagents on a millimeter-sized sample. *J Flow Chem*. 2020;10:615–625.
21. Parittotokkaporn S, Dravid A, Bansal M, et al. Make it simple: long-term stable gradient generation in a microfluidic microdevice. *Biomed Microdevices*. 2019;21(3):77.
22. Mo SJ, Lee JH, Kye HG, et al. A microfluidic gradient device for drug screening with human iPSC-derived motoneurons. *Analyst*. 2020;145(8):3081–3089.
23. Wolfram CJ, Rubloff GW, Luo X. Perspectives in flow-based microfluidic gradient generators for characterizing bacterial chemotaxis. *Biomicrofluidics*. 2016;10(6):061301.
24. Ebadi M, Moshksayan K, Kashaninejad N, Saidi MS, Nguyen N-T. A tool for designing tree-like concentration gradient generators for lab-on-a-chip applications. *Chem Eng Sci*. 2020;212:115339.
25. Tang Q, Li X, Lai C, et al. Fabrication of a hydroxyapatite-PDMS microfluidic chip for bone-related cell culture and drug screening. *Bioact Mater*. 2021;6(1):169–178.
26. Shimizu A, Goh WH, Itai S, Karyappa R, Hashimoto M, Onoe H. ECM-based microfluidic gradient generator for tunable surface environment by interstitial flow. *Biomicrofluidics*. 2020;14(4):044106.
27. Kang YB, Eo J, Mert S, Yarmush ML, Usta OB. Metabolic patterning on a chip: towards in vitro liver zonation of primary rat and human hepatocytes. *Sci Rep*. 2018;8(1):8951.
28. Hong B, Xue P, Wu Y, Bao J, Chuah YJ, Kang Y. A concentration gradient generator on a paper-based microfluidic chip coupled with cell culture microarray for high-throughput drug screening. *Biomed Microdevices*. 2016;18(1):21.
29. Wei Y, Zhu Y, Fang Q. Nanoliter quantitative high-throughput screening with large-scale tunable gradients based on a microfluidic droplet robot under unilateral dispersion mode. *Anal Chem*. 2019;91(8):4995–5003.
30. Xu Z, Fang P, Xu B, et al. High-throughput three-dimensional chemotactic assays reveal steepness-dependent complexity in neuronal sensation to molecular gradients. *Nat Commun*. 2018;9(1):4745.
31. Zhang Y, Xiao RR, Yin T, et al. Generation of gradients on a microfluidic device: toward a high-throughput investigation of spermatozoa chemotaxis. *PLoS One*. 2015;10(11):e0142555.
32. Ezra Tsur E, Zimmerman M, Maor I, Elrich A, Nahmias Y. Microfluidic concentric gradient generator design for high-throughput cell-based studies. *Front Bioeng Biotechnol*. 2017;5:21.
33. Mulholland T, McAllister M, Patek S, et al. Drug screening of biopsy-derived spheroids using a self-generated microfluidic concentration gradient. *Sci Rep*. 2018;8(1):14672.
34. Shen S, Zhang X, Zhang F, Wang D, Long D, Niu Y. Three-gradient constructions in a flow-rate insensitive microfluidic system for drug screening towards personalized treatment. *Talanta*. 2020;208:120477.
35. Lim W, Park S. A microfluidic spheroid culture device with a concentration gradient generator for high-throughput screening of drug efficacy. *Molecules*. 2018;23(12):3355.
36. Nakajima A, Ishida M, Fujimori T, Wakamoto Y, Sawai S. The microfluidic lighthouse: an omnidirectional gradient generator. *Lab Chip*. 2016;16(22):4382–4394.

37. Esch MB, Prot J-M, Wang YI, et al. Multi-cellular 3D human primary liver cell cultures elevate metabolic activity under fluidic flow. *Lab Chip*. 2015;15(10):2269–2277.
38. Bhushan A, Senutovitch N, Bale SS, et al. Towards a three-dimensional microfluidic liver platform for predicting drug efficacy and toxicity in humans. *Stem Cell Res Ther*. 2013;4(Suppl 1):S16.
39. Lin R-Z, Chang H-Y. Recent advances in three-dimensional multicellular spheroid culture for biomedical research. *Biotechnol J*. 2008;3(9–10):1172–1184.
40. Ziółkowska K, Kwapiszewski R, Brzózka Z. Microfluidic devices as tools for mimicking the in vivo environment. *New J Chem*. 2011;35(5):979–990.
41. Astolfi M, Péant B, Lateef MA, et al. Micro-dissected tumor tissues on chip: an ex vivo method for drug testing and personalized therapy. *Lab Chip*. 2016;16(2):312–325.
42. Hay M, Thomas DW, Craighead JL, Economides C, Rosenthal J. Clinical development success rates for investigational drugs. *Nat Biotechnol*. 2014;32(1):40–51.
43. Yin L, Du G, Zhang B, et al. Efficient drug screening and nephrotoxicity assessment on co-culture microfluidic kidney chip. *Sci Rep*. 2020;10(1):6568.
44. Mixtelena-Iribarren O, Zabalo J, Arana S, Mujika M. Improved microfluidic platform for simultaneous multiple drug screening towards personalized treatment. *Biosens Bioelectron*. 2019;123:237–243.
45. Quail DF, Joyce JA. Microenvironmental regulation of tumor progression and metastasis. *Nat Med*. 2013;19(11):1423–1437.
46. Floor SL, Dumont JE, Maenhaut C, Raspe E. Hallmarks of cancer: of all cancer cells, all the time? *Trends Mol Med*. 2012;18(9):509–515.
47. Virumbrales-Muñoz M, Ayuso JM, Olave M, et al. Multiwell capillarity-based microfluidic device for the study of 3D tumour tissue-2D endothelium interactions and drug screening in co-culture models. *Sci Rep*. 2017;7(1), 11998.
48. Wong CH, Siah KW, Lo AW. Estimation of clinical trial success rates and related parameters. *Biostatistics (Oxford, England)*. 2019;20(2):273–286.
49. Chi C-W, Lao Y-H, Ahmed AHR, et al. High-throughput tumor-on-a-chip platform to study tumor–stroma interactions and drug pharmacokinetics. *Adv Healthc Mater*. 2020. n/a(n/a):2000880.
50. Pradhan S, Smith AM, Garson CJ, et al. A microvascularized tumor-mimetic platform for assessing anti-cancer drug efficacy. *Sci Rep*. 2018;8(1):3171.
51. Siegel RL, Miller KD, Jemal A. Cancer statistics, 2017. *CA Cancer J Clin*. 2017;67(1):7–30.
52. Zhu P, Du XL, Lu G, Zhu J-J. Survival benefit of glioblastoma patients after FDA approval of temozolomide concomitant with radiation and bevacizumab: a population-based study. *Oncotarget*. 2017;8(27):44015–44031.
53. Akay M, Hite J, Avci NG, et al. Drug screening of human GBM spheroids in brain cancer chip. *Sci Rep*. 2018;8(1):15423.
54. Vatandoust S, Price TJ, Karapetis CS. Colorectal cancer: metastases to a single organ. *World J Gastroenterol*. 2015;21(41):11767–11776.
55. Carvalho MR, Lima D, Reis RL, Oliveira JM, Correlo VM. Anti-cancer drug validation: the contribution of tissue engineered models. *Stem Cell Rev Rep*. 2017;13(3):347–363.
56. Carvalho MR, Barata D, Teixeira LM, et al. Colorectal tumor-on-a-chip system: a 3D tool for precision onco-nanomedicine. *Sci Adv*. 2019;5(5):eaaw1317.
57. Weeber F, Ooft SN, Dijkstra KK, Voest EE. Tumor organoids as a pre-clinical cancer model for drug discovery. *Cell Chem Biol*. 2017;24(9):1092–1100.
58. Sabhachandani P, Motwani V, Cohen N, Sarkar S, Torchilin V, Konry T. Generation and functional assessment of 3D multicellular spheroids in droplet based microfluidics platform. *Lab Chip*. 2016;16(3):497–505.

59. Jung DJ, Shin TH, Kim M, Sung CO, Jang SJ, Jeong GS. A one-stop microfluidic-based lung cancer organoid culture platform for testing drug sensitivity. *Lab Chip*. 2019;19(17):2854–2865.
60. Llovet JM, Zucman-Rossi J, Pikarsky E, et al. Hepatocellular carcinoma. *Nat Rev Dis Primers*. 2016;2(1):16018.
61. Lu S, Cuzzucoli F, Jiang J, et al. Development of a biomimetic liver tumor-on-a-chip model based on decellularized liver matrix for toxicity testing. *Lab Chip*. 2018;18(22):3379–3392.
62. Bilal M, Mehmood S, Raza A, Hayat U, Rasheed T, Iqbal H. Microneedles in smart drug delivery. *Adv Wound Care (New Rochelle)*. 2020;10:204–219 [ja].
63. Yang J, Liu X, Fu Y, Song Y. Recent advances of microneedles for biomedical applications: drug delivery and beyond. *Acta Pharm Sin B*. 2019;9(3):469–483.
64. Lee K, Goudie MJ, Tebon P, et al. Non-transdermal microneedles for advanced drug delivery. *Adv Drug Deliv Rev*. 2019;165–166:41–59.
65. Rzhetskiy AS, Singh TRR, Donnelly RF, Anissimov YG. Microneedles as the technique of drug delivery enhancement in diverse organs and tissues. *J Control Release*. 2018;270:184–202.
66. Lee K, Lee J, Lee SG, et al. Microneedle drug eluting balloon for enhanced drug delivery to vascular tissue. *J Control Release*. 2020;321:174–183.
67. Lee K, Song HB, Cho W, Kim JH, Kim JH, Ryu W. Intracorneal injection of a detachable hybrid microneedle for sustained drug delivery. *Acta Biomater*. 2018;80:48–57.
68. Ng LC, Gupta M. Transdermal drug delivery systems in diabetes management: a review. *Asian J Pharm Sci*. 2020;15(1):13–25.
69. Azmana M, Mahmood S, Hilles AR, Mandal UK, Al-Japairai KAS, Raman S. Transdermal drug delivery system through polymeric microneedle: a recent update. *J Drug Deliv Sci Technol*. 2020;60, 101877.
70. Chen M, Quan G, Sun Y, Yang D, Pan X, Wu C. Nanoparticles-encapsulated polymeric microneedles for transdermal drug delivery. *J Control Release*. 2020;325:163–175.
71. Barnum L, Samandari M, Schmidt TA, Tamayol A. Microneedle arrays for the treatment of chronic wounds. *Expert Opin Drug Deliv*. 2020;17:1–14.
72. Moreira AF, Rodrigues CF, Jacinto TA, Miguel SP, Costa EC, Correia IJ. Microneedle-based delivery devices for cancer therapy: a review. *Pharmacol Res*. 2019;148:104438.
73. Kang N-W, Kim S, Lee J-Y, et al. Microneedles for drug delivery: recent advances in materials and geometry for preclinical and clinical studies. *Expert Opin Drug Deliv*. 2020;18:929–947.
74. Waghule T, Singhvi G, Dubey SK, et al. Microneedles: a smart approach and increasing potential for transdermal drug delivery system. *Biomed Pharmacother*. 2019;109:1249–1258.
75. Larraneta E, Lutton RE, Woolfson AD, Donnelly RF. Microneedle arrays as transdermal and intradermal drug delivery systems: materials science, manufacture and commercial development. *Mater Sci Eng: R: Rep*. 2016;104:1–32.
76. Sabri AH, Kim Y, Marlow M, et al. Intradermal and transdermal drug delivery using microneedles—fabrication, performance evaluation and application to lymphatic delivery. *Adv Drug Deliv Rev*. 2020;153:195–215.
77. Kashaninejad N, Munaz A, Moghadas H, Yadav S, Umer M, Nguyen N-T. Microneedle arrays for sampling and sensing skin interstitial fluid. *Chemosensors*. 2021;9(4):83.
78. Al-Japairai KAS, Mahmood S, Almurisi SH, et al. Current trends in polymer microneedle for transdermal drug delivery. *Int J Pharm*. 2020;587:119673.
79. Ita K. Ceramic microneedles and hollow microneedles for transdermal drug delivery: two decades of research. *J Drug Deliv Sci Technol*. 2018;44:314–322.

80. Nagarkar R, Singh M, Nguyen HX, Jonnalagadda S. A review of recent advances in microneedle technology for transdermal drug delivery. *J Drug Deliv Sci Technol.* 2020;59:101923.
81. Ali R, Mehta P, Arshad M, Kucuk I, Chang M, Ahmad Z. Transdermal microneedles—a materials perspective. *AAPS PharmSciTech.* 2020;21(1):12.
82. Yang H, Wu X, Zhou Z, Chen X, Kong M. Enhanced transdermal lymphatic delivery of doxorubicin via hyaluronic acid based transfersomes/microneedle complex for tumor metastasis therapy. *Int J Biol Macromol.* 2019;125:9–16.
83. Parhi R, Divya Supriya N. Review of microneedle based transdermal drug delivery systems. *Int J Pharm Sci Nanotech.* 2019;12(3):4511–4523. <https://doi.org/10.37285/ijpsn.2019.12.3.1>.
84. Ingrole RS, Gill HS. Microneedle coating methods: a review with a perspective. *J Pharmacol Exp Ther.* 2019;370(3):555–569.
85. Li L, Eyckmans J, Chen CS. Designer biomaterials for mechanobiology. *Nat Mater.* 2017;16(12):1164–1168.
86. Chandrasekharan A, Hwang YJ, Seong K-Y, Park S, Kim S, Yang SY. Acid-treated water-soluble chitosan suitable for microneedle-assisted intracutaneous drug delivery. *Pharmaceutics.* 2019;11(5):209.
87. Lopez-Ramirez MA, Soto F, Wang C, et al. Built-in active microneedle patch with enhanced autonomous drug delivery. *Adv Mater.* 2020;32(1), 1905740.
88. Thakur RRS, Tekko IA, Al-Shammari F, Ali AA, McCarthy H, Donnelly RF. Rapidly dissolving polymeric microneedles for minimally invasive intraocular drug delivery. *Drug Deliv Transl Res.* 2016;6(6):800–815.
89. Chen C-H, Shyu VB-H, Chen C-T. Dissolving microneedle patches for transdermal insulin delivery in diabetic mice: potential for clinical applications. *Materials (Basel).* 2018;11(9):1625.
90. Leone M, Mönkäre J, Bouwstra J, Kersten G. Dissolving microneedle patches for dermal vaccination. *Pharm Res.* 2017;34(11):2223–2240.
91. GhavamiNejad A, Li J, Lu B, et al. Glucose-responsive composite microneedle patch for hypoglycemia-triggered delivery of native glucagon. *Adv Mater.* 2019;31(30):1901051.
92. Ita K. Dissolving microneedles for transdermal drug delivery: advances and challenges. *Biomed Pharmacother.* 2017;93:1116–1127.
93. Nguyen HX, Bozorg BD, Kim Y, et al. Poly (vinyl alcohol) microneedles: fabrication, characterization, and application for transdermal drug delivery of doxorubicin. *Eur J Pharm Biopharm.* 2018;129:88–103.
94. Chen Y, Yang Y, Xian Y, et al. Multifunctional graphene-oxide-reinforced dissolvable polymeric microneedles for transdermal drug delivery. *ACS Appl Mater Interfaces.* 2019;12(1):352–360.
95. Luo Z, Sun W, Fang J, et al. Biodegradable gelatin methacryloyl microneedles for transdermal drug delivery. *Adv Healthc Mater.* 2019;8(3):1801054.
96. Luzuriaga MA, Berry DR, Reagan JC, Saldone RA, Gassensmith JJ. Biodegradable 3D printed polymer microneedles for transdermal drug delivery. *Lab Chip.* 2018;18(8):1223–1230.
97. Zhu DD, Wang QL, Liu XB, Guo XD. Rapidly separating microneedles for transdermal drug delivery. *Acta Biomater.* 2016;41:312–319.
98. Zhuang J, Rao F, Wu D, et al. Study on the fabrication and characterization of tip-loaded dissolving microneedles for transdermal drug delivery. *Eur J Pharm Biopharm.* 2020;157:66–73.
99. Jayaneththi V, Aw K, Sharma M, Wen J, Svirskis D, McDaid A. Controlled transdermal drug delivery using a wireless magnetic microneedle patch: preclinical device development. *Sensors Actuators B Chem.* 2019;297:126708.

100. Queiroz MLB, Shanmugam S, Santos LNS, et al. Microneedles as an alternative technology for transdermal drug delivery systems: a patent review. *Expert Opin Ther Pat.* 2020;30(6):433–452.
101. Gao Y, Hou M, Yang R, et al. Highly porous silk fibroin scaffold packed in PEGDA/sucrose microneedles for controllable transdermal drug delivery. *Biomacromolecules.* 2019;20(3):1334–1345.
102. Prausnitz MR. Engineering microneedle patches for vaccination and drug delivery to skin. *Ann Rev Chem Biomol Eng.* 2017;8:177–200.
103. Sharma S, Hatware K, Bhadane P, Sindhikar S, Mishra DK. Recent advances in microneedle composites for biomedical applications: advanced drug delivery technologies. *Mater Sci Eng C.* 2019;103:109717.
104. Dal Dosso F, Kokalj T, Belotserkovsky J, Spasic D, Lammertyn J. Self-powered infusion microfluidic pump for ex vivo drug delivery. *Biomed Microdevices.* 2018;20(2):44.
105. Maleki MA, Soltani M, Kashaninejad N, Nguyen N-T. Effects of magnetic nanoparticles on mixing in droplet-based microfluidics. *Phys Fluids.* 2019;31(3):032001.
106. Yaghoobi M, Saidi MS, Ghadami S, Kashaninejad N. An interface–particle interaction approach for evaluation of the co-encapsulation efficiency of cells in a flow-focusing droplet generator. *Sensors.* 2020;20(13):3774.
107. Maleki MA, Zhang J, Kashaninejad N, Soltani M, Nguyen N-T. Magnetofluidic spreading in circular chambers under a uniform magnetic field. *Microfluid Nanofluid.* 2020;24(10):80.